NEOPLASIA
www.neoplasia.com

Volume 19 Number 9 September 2017 pp. 661–671 661

The Antitumor Activity of IMGN529, a CD37-Targeting Antibody-Drug Conjugate, Is Potentiated by Rituximab in Non-Hodgkin Lymphoma Models

Stuart W. Hicks, Katharine C. Lai, L. Cristina Gavrilescu, Yong Yi, Surina Sikka, Prerak Shah, Meghan E. Kelly, Jenny Lee, Leanne Lanieri, Jose F. Ponte, Callum M. Sloss and Angela Romanelli

ImmunoGen, Inc., Waltham, MA

Abstract

Naratuximab emtansine (IMGN529) is an investigational antibody-drug conjugate consisting of a CD37-targeting antibody conjugated to the maytansine-derived microtuble disruptor, DM1. IMGN529 has shown promising preclinical and clinical activity in non-Hodgkin lymphoma, including diffuse large B-cell lymphoma (DLBCL). Due to the aggressive nature of the disease, DLBCL is often treated with combination therapies to maximize clinical outcomes; therefore, we investigated the potential of combining IMGN529 with both standard-of-care and emerging therapies against multiple oncology-relevant targets and pathways. The strongest enhancement in potency was seen with anti-CD20 antibodies, including rituximab. The combination of IMGN529 and rituximab was more potent than either agent alone, and this combinatorial benefit was associated with increased apoptotic induction and cell death. Additional studies revealed that rituximab treatment increased the internalization and degradation of the CD37-targeting antibody moiety of IMGN529. The combination of IMGN529 and rituximab was highly efficacious in multiple xenograft models, with superior antitumor efficacy seen compared to either agent alone or treatment with R-CHOP therapy. These findings suggest a novel mechanism whereby the potency of IMGN529 can be enhanced by CD20 binding, which results in the increased internalization and degradation of IMGN529 leading to the generation of greater amounts of cytotoxic catabolite. Overall, these data provide a biological rationale for the enhanced activity of IMGN529 in combination with rituximab and support the ongoing clinical evaluation of IMGN529 in combination with rituximab in patients with relapsed and/or refractory DLBCL.

Neoplasia (2017) 19, 661–671

Introduction

Despite the availability of a wide variety of therapeutic agents and the success of the addition of the anti-CD20 antibody rituximab to front-line chemotherapy, up to one third of patients with aggressive non-Hodgkin lymphoma (NHL), in particular diffuse large B-cell lymphoma (DLBCL), relapse following initial treatment or are refractory to current therapies. In response to this unmet need, recent efforts have focused on the development of new antibodies to improve overall survival including the characterization of alternative B-cell surface antigens (e.g., CD19, CD22, CD30) that may potentially serve as novel targets for therapeutic intervention [1,2].

One antigen of considerable interest is the tetraspanin CD37, a transmembrane protein proposed to function in immune cell proliferation and survival [3,4]. In normal lymphoid tissues, CD37 shows a restricted expression profile, limited primarily to mature B

Abbreviations: ADC, antibody-drug conjugate; NHL, non-Hodgkin lymphoma; *DLBCL*, diffuse large B-cell lymphoma; ADCC, antibody-dependent cell-mediated cytotoxicity; CDC, complement-dependent cytotoxicity; MMAE, monomethyl auristatin E; SMCC, N-succinimidyl-4-(N-maleimidoethyl) cyclohexane-1-carboxylate; GI, Growth Inhibition; CPM, counts per minute; PR, partial tumor regression; CR, complete response; TFS, tumor free survivors; ABC, activated B-cell; GCB, germinal B-cell.

Address all correspondence to: Stuart W. Hicks, Discovery Research, ImmunoGen Inc., 830 Winter St, Waltham, MA 02451.
E-mail: stuart.hicks@immunogen.com

Received 2 May 2017; Revised 15 June 2017; Accepted 15 June 2017

1476-5586
http://dx.doi.org/10.1016/j.neo.2017.06.001

cells from the pre-B through peripheral stages of differentiation and absent from plasma cells [5,6]. In addition, CD37 is highly expressed on the surface of malignant B cells, including most subtypes of NHL [7,8]. This expression pattern has prompted the development of a number of CD37-targeting therapeutics, including otlertuzumab (TRU-016; a CD37-binding, single-chain homodimeric protein) [9] and BI 836826 (an Fc-engineered antibody) [10], both of which act *via* antibody-dependent cell-mediated cytotoxicity (ADCC) and apoptotic signaling. Each of these agents has now entered clinical testing, but to date, only modest activity has been reported from the initial human trials with otlertuzumab [11,12].

The expression of CD37 on transformed B cells makes it an attractive target for development of antibody-drug conjugate (ADC) therapy. ADCs are designed to deliver chemotherapeutics to tumor cells by linking highly potent small molecules to monoclonal antibodies that recognize tumor-associated antigens, with the goal of improving antitumor activity while reducing systemic toxicity [13]. This approach has been validated in both the hematological and solid tumor settings, as evidenced by FDA approval of two ADCs: brentuximab vedotin (Adcetris), a conjugate of an anti-CD30 antibody with monomethyl auristatin E (MMAE) [14], in relapsed Hodgkin lymphoma and systemic anaplastic large-cell lymphoma, and ado-trastuzumab emtansine (Kadcyla), a conjugate of trastuzumab with the maytansinoid DM1 [15] used to treat patients with HER2-positive metastatic breast cancer. We are developing naratuximab emtansine (IMGN529), an ADC comprised of DM1 linked to a humanized anti-CD37 antibody *via* the same linker used in Kadcyla, as a new investigational agent that effectively combines the intrinsic proapoptotic and effector activities of its antibody component with the cytotoxic activity of the maytansinoid payload [16]. In this manner, IMGN529 can be distinguished from another CD37-targeting ADC, AGS67E, which consists of MMAE linked to an antibody moiety that lacks any intrinsic apoptotic or ADCC activity [17]. IMGN529 binds with high affinity and specificity to CD37, which allow for ADC internalization, processing, and intracellular release of DM1. As a result of its ability to disrupt microtubule assembly, DM1 subsequently induces cell cycle arrest and apoptosis.

IMGN529 has shown robust antitumor activity in preclinical models of CD37-positive NHL [16,18], which led to its clinical evaluation in the treatment of B-cell malignancies. Importantly, the first-in-human phase I trial of IMGN529 conducted in patients with relapsed or refractory B-cell NHL revealed a manageable safety profile and encouraging evidence of single-agent efficacy, particularly in individuals with DLBCL [19]. Here we report that the activity of IMGN529 is significantly enhanced when combined with anti-CD20 antibodies. The findings presented here are of considerable translational relevance for the continued clinical development of IMGN529 as an effective cancer therapeutic.

Materials and Methods

Antibodies and ADC Generation

The humanized anti-CD37 antibody K7135A and nontargeting control IgG of the same isotype and identical Fc sequence were generated at ImmunoGen. The anti-CD19 (huB4) and anti-CD22 (huBU59) antibodies were produced by transient transfection in HEK 293T cells at ImmunoGen. The anti-CD20 antibodies rituximab, ofatumumab, and obinutuzumab were obtained from commercial sources. IMGN529 and the control nontargeting IgG1-SMCC-DM1 conjugate were produced *via* conjugation of the maytansinoid DM1 to the K7153A and the nontargeting IgG1 antibodies, respectively, using the cross-linking agent *N*-succinimidyl-4-(*N*-maleimidoethyl) cyclohexane-1-carboxylate (SMCC) as described previously [16].

Combination Screen

High-throughput combination screens were performed by Horizon CombinatoRx Inc. (Cambridge, MA) to examine IMGN529 activity in combination with 104 compounds. The combination screen was performed in 20 NHL cell lines. Briefly, each cell line was cultured and plated in optimal conditions based on growth characteristics in 384- or 1536-well tissue culture plates. Compounds were added to assay plates using a 6×6 or 6×8 dose matrix of IMGN529 and each combination agent. Concentration ranges were selected based on single agent activity of each molecule on a panel of cell lines. Cell viability was evaluated using an ATPLite assay (Perkin Elmer) following 72 hours of treatment. In addition to IMGN529, the combination activities for K7153A, IgG1-SMCC-DM1 (nontargeting ADC), and unconjugated DM1-Me were determined. All data points were collected *via* automated processes, quality controlled, and analyzed using Horizon CombinatoRx proprietary Chalice software.

Horizon utilizes growth inhibition (GI) as a measure of cell viability. GI is calculated by applying the following test and equation:

$$\text{If } T < V_0 : 100^*(1-(T-V_0)/V_0)$$

$$\text{If } T \geq V_0 : 100^*(1-(T-V_0)/(V-V_0))$$

where T is the signal for a test agent after 72 hours, V is the vehicle-treated control measure at 72 hours, and V_0 is the vehicle control measure at time zero.

A GI reading of 0% represents no growth inhibition where cells treated with compound (T) and (V) vehicle signals are the same. A GI of 100% represents complete growth inhibition or cytostatic conditions where cells treated by compound match the signal of V_0. Compounds reaching GI 200% are considered cytotoxic and represent complete cell death.

To quantitate the combination effects in excess of Loewe additivity, a scalar measure was used to characterize the strength of synergistic interaction termed the Synergy Score.

$$\text{Synergy Score} = \log f_X \log f_Y \Sigma \max(0, \text{Idata})(\text{Idata}-\text{ILoewe})$$

The Synergy Score equation integrates the experimentally observed activity volume at each point in the matrix in excess of a model surface numerically derived from the activity of the component agents using the Loewe model for additivity. Additional terms in the Synergy Score equation are used to normalize for various dilution factors used for individual agents and to allow for comparison of synergy scores across the entire experiment.

Cell Lines

For studies performed at ImmunoGen, the U-2932, SU-DHL-4, DOHH-2, OCI-Ly18, and OCI-Ly7 lines were obtained from DSMZ; the Farage cell line was purchased from ATCC. All lines were characterized by the vendor using routine DNA profiling; no further

authentication was performed by the authors. Cells were expanded and maintained as recommended in a humidified 37 °C, 5% CO_2 incubator. All cell lines show membrane expression of both CD20 and CD37.

Apoptosis Assays

Apoptosis was assessed using the luminescence-based Caspase-Glo 3/7 assay kit (Promega) according to manufacturers' instructions. Exponentially growing DLBCL cell lines were seeded into 96-well plates and incubated in the presence of previously determined saturating concentrations of IMGN529 or rituximab, both alone and in combination, for 24 hours. Caspase-Glo 3/7 reagent was added (50% v/v) to the cells, and plates were incubated for 30 minutes before luminescence detection in a Victor3 microplate reader (PerkinElmer). Additional caspase3/7 activation studies were performed combining IMGN529 with ofatumumab, obinutuzumab, K7153A, and IgG1-SMCC-DM1 in the U-2932 and SU-DHL-4 cell lines using the same protocol.

Western Blotting

Cells were incubated with 20 μg/ml rituximab, 1 nM IMGN529, or the combination for 24 hours. Cellular extracts were prepared and proteins resolved by sodium dodecyl sulfate polyacrylamide gel electrophoresis before transfer to polyvinylidene fluoride membranes. After blocking, membranes were simultaneously incubated with rabbit anti-cleaved PARP, mouse anti–β-actin, and mouse anti-GAPDH antibodies (Cell Signaling Technology). Bound antibodies were detected using an anti-rabbit peroxidase-conjugated secondary antibody (Cell Signaling Technology) and an anti-mouse Alexa-Fluor 680–conjugated secondary antibody (Thermo Fisher Scientific). Chemiluminescent detection was performed using Super-Signal West Dura Extended Duration Substrate (Thermo Fisher Scientific). Both chemiluminescent detection and fluorescent detection were visualized using the ChemiDoc MP imaging system (Bio-Rad, USA).

ADCC and Complement-Dependent Cytotoxicity (CDC) Assays

ADCC activity was measured using 2.5×10^4 target cells and purified human natural killer cells (1:3 or 1:4 ratio) by lactate dehydrogenase release (Cytotoxicity Detection Kit; Roche) after a 4-hour incubation. The percentage of specific lysis was determined as % lysis = (experimental release − spontaneous release)/(maximum release − spontaneous release) × 100. For the CDC assays, antibodies or conjugates were incubated with 5×10^4 target cells/well and 5% human complement (Sigma-Aldrich) for 2 hours. Cell viability was assessed by alamarBlue assay (Invitrogen).

Flow Cytometry-Based Internalization

For internalization studies, K7153A- and rituximab-Alexa488 antibody conjugates were generated using Alexa Fluor 488 tetrafluorophenyl ester according to the manufacturer's instructions (Thermo Fisher). The conjugates were eluted in sodium azide free PBS, pH 7.2, to enable internalization assays. FACS binding assays were performed to ensure that Alexa488-labeling did not adversely affect target binding. K7153A-AF488 was added to exponentially growing cultures of U-2932 or SU-DHL-4 cells in 96-well plates in the presence or absence of 10 nM rituximab, ofatumumab, obinutuzumab, or control IgG. The plates were incubated on ice for 30 minutes or at 37°C for 30 minutes, 2 hours, and 6 hours. Cells were washed with ice-cold PBS twice, and replicate wells were resuspended in ice-cold PBS without (unquenched samples) or with an excess of anti-AF488 antibody (quenched samples). All samples were incubated for 30 minutes on ice. Cells were then fixed in 1% formaldehyde in PBS, and fluorescence was read by flow cytometry. The internalization of rituximab-AF488 either alone or in the presence of K7153A or anti-CD19 antibody was measured using the same methodology. The fluorescence of cells incubated on ice for 30 minutes in the presence of anti-Alexa488 antibody represents the unquenchable fluorescent fraction and was subtracted from all other samples prior to calculating internalization. The percent internalization was calculated as the intracellular fluorescence (the fluorescence of quenched samples corrected for incomplete surface quenching) divided by the total fluorescence (the fluorescence of unquenched cells minus the autofluorescence of cells).

Antibody Processing Studies

K7153A and anti-CD19 (huB4) monoclonal antibodies were labeled at lysine residues with *N*-succinimidyl-[2,3,3H]propionate (ARC, Inc.) as previously described [20]. U-2932 and SU-DHL-4 cells were exposed for a 30-minute pulse with 10 nM of ^{3}H-propionamide–labeled K7153A antibody (^{3}H-K7153A) in the presence or absence of rituximab, anti-CD19, anti-CD22, or nontargeting IgG1 antibodies. Some samples were preblocked with 500 nM (50-fold excess) of unlabeled antibodies for 15 minutes prior to ^{3}H-Ab treatment. Cell lines were also pulse labeled with ^{3}H-huB4 with or without rituximab cotreatment to measure the generation of anti-CD19 catabolite formation. Cells were washed and cultured for 24 hours prior to harvest and extraction to separate soluble ^{3}H species from protein-associated species. Radioactivity was measured by liquid scintillation counting using a Tri-Carb 2900T counter (Packard BioScience,) and calculated based on counts per minute (CPM) values. Antibodies bound per cell values for both cell lines were determined from the tritium CPM of both extract and pellet fractions using the following equation: ((CPMextract + CPMpellet) / # cells) × (1 dpm/0.6 dpm) × (1 mCi/2.2 × 10^9dpm) × (1 mmol/conjugate Ci) × (1 mol/1000 mmol) × (1 Ci/1000 mCi) × (6.022 × 10^{23} antigen binding sites/1 mol cells) × (1 antibody/1 antigen binding site). The percentage of ^{3}H-Ab conjugate processed was determined from the following equation: CPMextract/(CPMextract + CPMpellet) × 100%. The picomoles of ^{3}H-catabolite per million cells value were determined by multiplying the CPM value of the protein-free extract per 1 million cell sample × (1 dpm/0.6 cpm) × (1 mCi/2.2 × 10^9 dpm) × (1 Ci/1000 mCi) × (1 mmol/conjugate Ci) × (1 × 10^9 pmol/1 mmol).

In Vivo Xenograft Models

All animal procedures were performed in strict accordance with ImmunoGen's Animal Care and Use Committee and the NIH Guide for the Care and Use of Laboratory Animals. Female CB.17-SCID mice (Charles River Laboratories) were inoculated subcutaneously on the right flank with U2932, SU-DHL-4, or OCI-Ly18 cells (10^7 cells/mouse). Animals were randomized into treatment groups (8 mice/group) at the time the mean tumor volume of the cohort reached ~100 mm^3. In the Farage model of disseminated disease, mice were tail vein injected with 10^7 Farage cells. Animals (10 mice/group) were randomized based on weight 7 days postinoculation. IMGN529 was administered as a single bolus of 2.5, 5, or 10 mg/kg. Rituximab was dosed at 10 mg/kg either as a single administration or as three consecutive weekly doses (QW×3) as indicated in the legends. R-CHOP therapy, used for comparative purposes, consisted of a

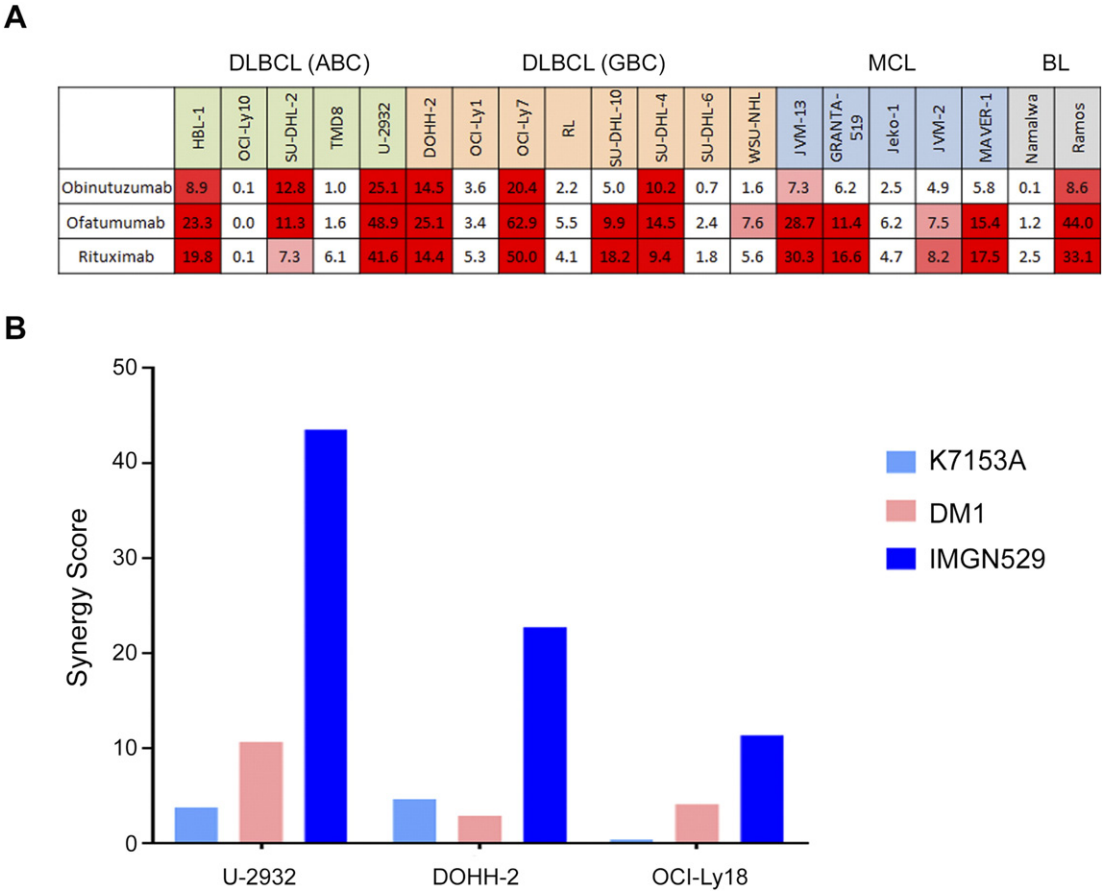

Figure 1. Synergy screening identifies combinatorial benefit between IMGN529 and anti-CD20 antibodies, which requires the intact ADC. (A) Heat map of synergy values for IMGN529 in combination with anti-CD20 antibodies. The cell line panel included ABC DLBCL (green), GCB DLBCL (orange), MCL (blue), and BL (gray) lines. (B) Synergy scores for rituximab in combination with the K7153A antibody, free DM1, or intact IMGN529 evaluated in U-2932, DOHH-2, and OCI-Ly18 cells.

single i.v. injection of 10 mg/kg rituximab, 30 mg/kg cyclophosphamide, 2.5 mg/kg doxorubicin, 0.375 mg/kg vincristine, and 0.15 mg/kg prednisone p.o. QD×5. For the subcutaneous xenograft models, tumor volume (TV) was recorded twice weekly by caliper measurements of the height (*H*), length (*L*), and width (*W*) of the tumor, following the formula TV = ($H \times L \times W$)/2. Tumor growth inhibition (TGI), a measure of efficacy, was expressed as a percentage of growth inhibition of tumors in the treatment group compared to the control (vehicle) group, following the formula TGI = $T/C \times 100$, where *T* is the median TV of the treated group when the control group's median reaches 1000 mm^3 (*C*). A partial tumor regression (PR) was scored for a mouse when the TV at any given measurement point was <50% of the initial TV pretreatment; a complete tumor regression (CR) was scored when no palpable tumor could be detected. Animals with a CR that lasted until the end of study were further classified as tumor-free survivors (TFS). For the disseminated model, animal survival was followed for 120 days; animals were removed from the study when advanced health distress signs were observed or measured (>20% loss of body weight, hind leg paralysis, tumor growth on body, or moribund state).

Results

Synergy Screening for Enhancers of IMGN529 Cytotoxicity

A broad *in vitro* screening approach was used to identify agents that enhanced the cytotoxic activity of IMGN529 in NHL cell lines. A combination screen was performed in 20 cell lines representing three NHL histotypes: DLBCL, including both activated B cell (ABC) and the germinal B cell (GCB) subtypes, mantle cell lymphoma (MCL), and Burkitt's lymphoma (BL). IMGN529 was combined with 104 oncocentric compounds, including standard-of-care and investigational therapeutics, using combination dose-response matrices. Tumor cell killing was assayed after 72 hours of treatment. Overall, 2080 unique combination pairings were generated. Combination synergies were identified when the cytotoxic activity of the combination superseded the baseline additive response (self-cross activity) by at least two standard deviations. While a number of agents showed synergistic tumor cell killing when combined with IMGN529, the most potent combination effects were observed with anti-CD20 antibodies including rituximab, ofatumumab, and obinutuzumab (Figure 1*A*). These synergy scores were up to six-fold higher than what was seen with other classes of agents. Due to the strong synergy seen with anti-CD20 antibodies and signals of activity of single-agent IMGN529 seen in DLBCL patients in the Phase I study, we prioritized the combination of IMGN529 with rituximab for additional preclinical studies in DLBCL models.

IMGN529 Plus Rituximab Synergy

The humanized monoclonal antibody K7153A used as the CD37-targeting moiety of IMGN529 was originally selected for

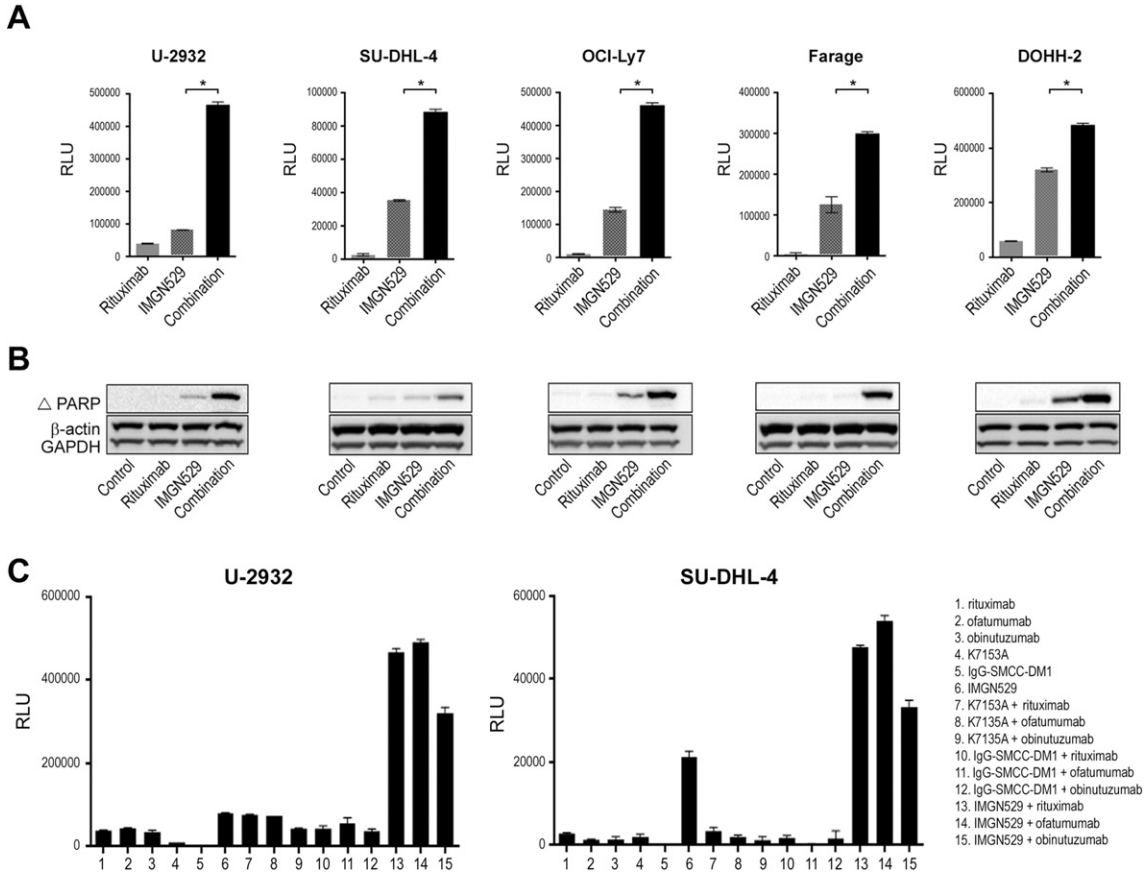

Figure 2. Combination IMGN529 and anti-CD20 antibody treatment induces apoptosis in DLBCL cell lines. (A) Caspase 3/7 activation in DLBCL cell lines following overnight exposure to 2 nM rituximab or 0.125 nM IMGN529, alone and in combination. *$P < .0001$ (unpaired *t* test). (B) Western blot analysis of cleaved PARP expression in the same panel of lines treated with rituximab, IMGN529, or the combination for 24 hours; β-actin and GAPDH are included as loading controls. (C) Caspase 3/7 activation in U-2932 and SU-DHL-4 cells was determined following overnight exposure to anti-CD20 antibodies, K7153A, IgG1-SMCC-DM1, or IMGN529, alone and in combination as indicated.

ADC development due to strong functional antibody activities, including apoptotic induction [16]. Therefore, we examined the respective contributions of the antibody and payload components, as well as the complete ADC molecule, to the synergistic interaction with rituximab in a subset of DLBCL cell lines (Figure 1*B*). Interestingly, neither K7153A nor the DM1 cytotoxic payload alone produced striking synergistic effects with rituximab; synergy was only observed when cells were exposed to the intact IMGN529 ADC in combination with the anti-CD20 antibody, suggesting that the combinatorial benefit requires CD37-targeted delivery of DM1.

Combinations of IMGN529 with Anti-CD20 Antibodies

To examine whether the induction of apoptosis contributed to the improved cytotoxicity, caspase 3/7 activation was measured in a panel of DLBCL cell lines treated with IMGN529 both alone and in combination with rituximab (Figure 2*A*). In each of the lines tested, single-agent rituximab treatment had negligible effects on caspase activity. In contrast, caspase 3/7 activation was induced following exposure to IMGN529, and this effect was significantly enhanced in the presence of rituximab. Combination treatment also induced a concomitant increase in the levels of cleaved PARP, another marker of cells undergoing apoptosis (Figure 2*B*). Taken together, these data indicated that CD20 engagement amplified the proapoptotic activity of IMGN529.

To extend this observation, multiple control and combination treatments were evaluated in U-2932 and SU-DHL-4 cells, representing both the ABC and GCB subtypes of DLBCL, respectively (Figure 2*C*). Single-agent exposure to the anti-CD20 antibodies, K7153A, or a nontargeting IgG1-SMCC-DM1 ADC had minimal effects on caspase 3/7 activation in either cell line. In agreement with Figure 1*C*, cotreatment of any of the anti-CD20 antibodies with the K7153A antibody or the control ADC failed to induce apoptosis. Similar to rituximab, the anti-CD20 antibodies ofatumumab and obinutuzumab each enhanced caspase activation in combination with IMGN529, further supporting an anti-CD20 class effect. These findings additionally underscored the requirement for targeted delivery of DM1 to tumor cells in order to achieve synergistic tumor killing effects.

Combinatorial Effects on Immune Effector Activity

Immune effector activities, such as ADCC, are also important mechanisms for the antitumor effects of both IMGN529 and rituximab [16,21]. *In vitro*, IMGN529 demonstrated dose-dependent ADCC activity against U-2932 and SU-DHL-4 cell lines (Figure 3*A*). The ADCC activity was further increased in the presence of increasing concentrations of rituximab but not a nontargeting IgG1 (Figure 3*B*).

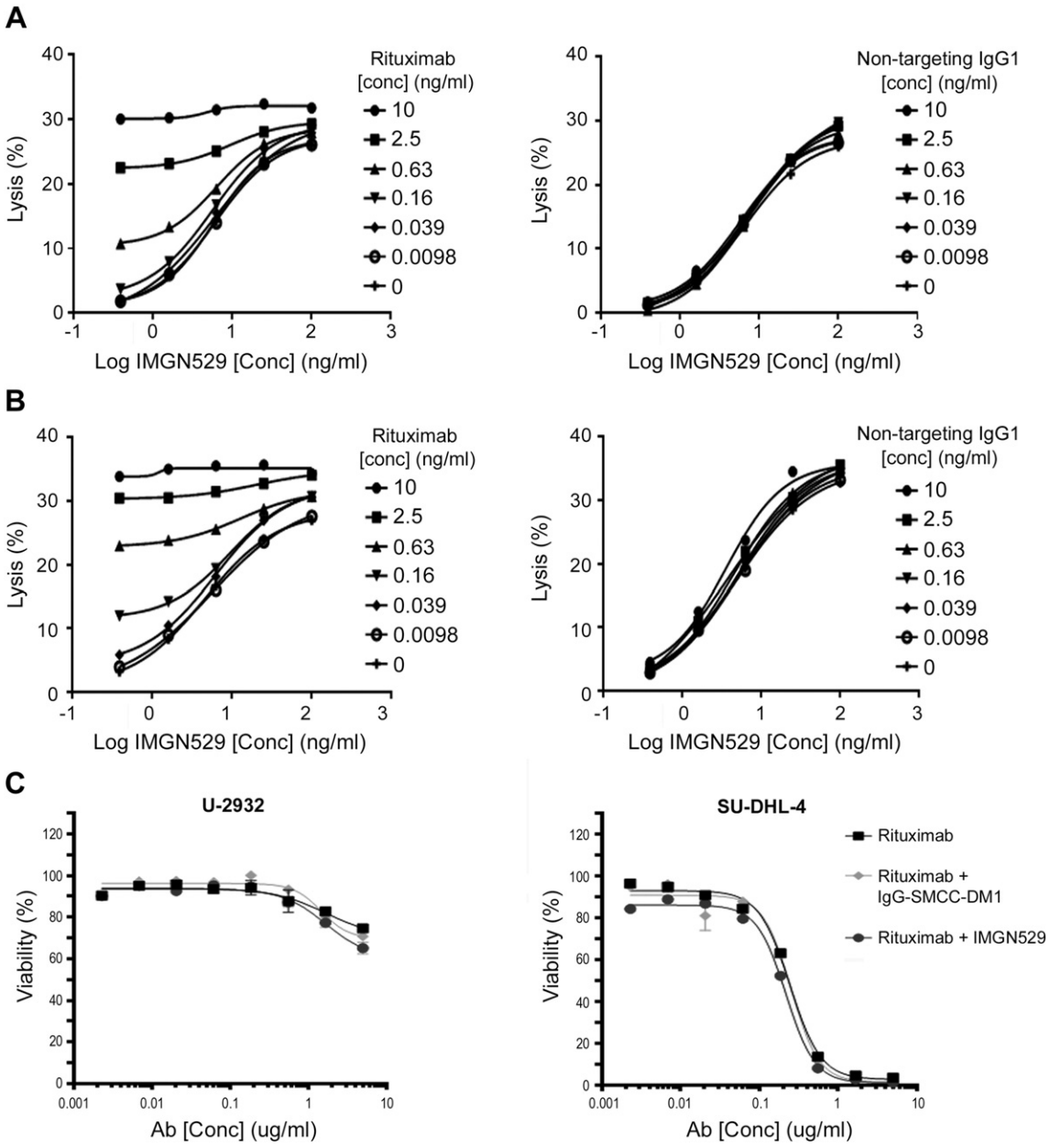

Figure 3. ADCC, but not CDC, is augmented by the combination of IMGN529 and rituximab. ADCC assays were performed by incubating target U-2932 (A) or SU-DHL-4 (B) cells with human NK effector cells at E/T ratio of 3:1 or 4:1 and measuring LDH release. Cells were exposed to increasing concentrations of IMGN529 in the presence or absence of varying concentrations of rituximab or control IgG, as indicated. Percent specific lysis was calculated, and data shown are the mean of three experiments. (C) CDC activity against U-2932 cells (*left panel*) and SU-DHL-4 cells (*right panel*) was determined following incubating cells for 2 hours with increasing concentrations of rituximab +/− 5 μg/mL of IMGN529 or IgG1-SMCC-DM1 in the presence of human complement. Cell viability was assessed by alamarBlue assay.

In addition, rituximab has been shown to activate complement and elicit CDC [16,21]. IMGN529 did not adversely affect the inherent CDC activity of rituximab itself (Figure 3*C*), suggesting that this mechanism of tumor elimination is preserved.

Effect of Rituximab on Anti-CD37 Antibody Internalization

The potency of ADCs, such as IMGN529, relies on the internalization, intracellular trafficking, and degradation of the ADC leading to release of the cytotoxic payload. Therefore, we investigated the effect of rituximab treatment on the internalization of the K7153A antibody, the targeting component of IMGN529. U-2932 and SU-DHL-4 cells were incubated with fluorescently labeled K7153A (K7153A-AF488) either alone or in combination with rituximab or a nontargeting IgG1 (Figure 4*A*). In both cell lines, the internalization of K7153A was similar whether incubated alone or with the control antibody. However, when cells were coincubated with K7153A-AF488 and rituximab, the internalization of K7153A increased by as much as three-fold, an effect that was discernable within 30 minutes. Similar results were obtained with ofatumumab and obinutuzumab. Importantly, preincubation of labeled K7153A

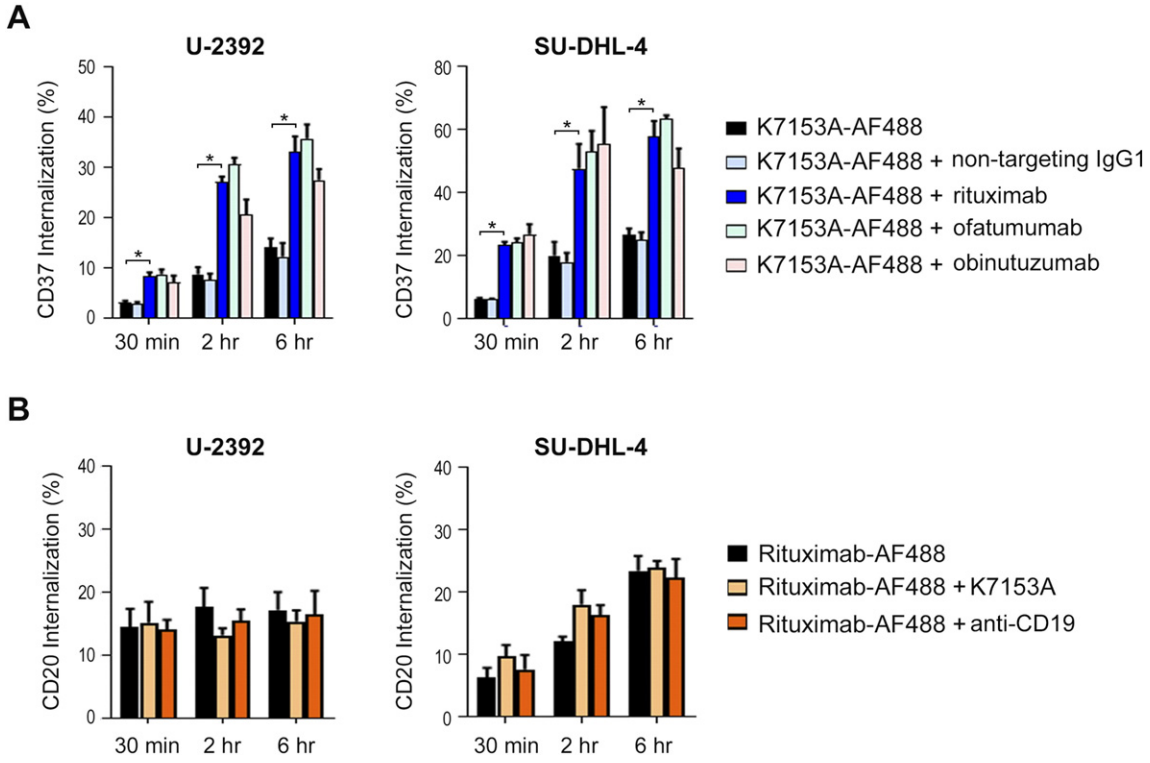

Figure 4. Rituximab cotreatment increases the internalization of the CD37-targeting moiety of IMGN529. (A) U-2932 cells (*left panel*) and SU-DHL-4 cells (*right panel*) cells were incubated with AF488-labeled K7153A in the presence or absence of the indicated control or anti-CD20 antibodies at 37°C for 30 minutes, 2 hours, and 6 hours. The percent internalization was determined by flow cytometry (*$P < .0001$, unpaired *t* test). (B) The internalization of AF488-labeled rituximab was determined alone or in the presence of K7153A or anti-CD19 antibodies in U-2932 (*left panel*) and SU-DHL-4 cells (*right panel*) cells.

with all three anti-CD20 antibodies yielded similar results to those seen with cotreatment, suggesting that the sequence of addition had no effect on the process (data not shown). Conversely, the addition of K7153A to fluorescently tagged rituximab (rituximab-AF488) had no impact on rituximab internalization (Figure 4*B*). Taken together, these data suggest that the anti-CD20 effect on K7153A is unidirectional and not mediated by antibody-antigen cross-linking leading to internalization.

Effect of Rituximab on Radiolabeled K7153A Degradation

Next, radiolabeled processing studies were performed to determine whether the enhanced internalization led to a corresponding increase in antibody degradation, necessary for the release of the cytotoxic payload of IMGN529. In order to evaluate lysosomal degradation, the CD37-targeting K7153A antibody was radiolabeled with ^{3}H-propionate. We have previously shown that ^{3}H-propionamide–labeled antibodies are processed to generate a ^{3}H-propionamido-lysine catabolite that correlates well with the known lysine-N^{ε}-SMCC-DM1 catabolite [20].

We first evaluated the potential modulation of CD37 expression by ^{3}H-K7153A binding when incubated with rituximab or other B-cell–targeting antibodies (Figure 5*A*). The CD37 antigen levels on the U-2932 and SU-DHL-4 cell lines (192,098 and 216,506 antibodies bound per cell, respectively) were consistent to those reported based on flow cytometry experiments [18]. Cotreatment with rituximab as well as anti-CD19, anti-CD22, or nontargeting IgG1 antibodies did not affect the amount of K7153A binding (Figure 5*A*), indicating that the observed increased internalization was not due to changes in CD37 expression on the cell surface.

Following pulse exposure with ^{3}H-K7153A, the mean percentage of K7153A degraded for U-2932 and SU-DHL-4 was 14% and 8%, respectively, after 20- to 24-hour incubation. A similar percentage of ^{3}H-K7153A degradation was seen with anti-CD19, anti-CD22, or nontargeting IgG1 antibodies. However, when combined with rituximab, this percentage increased to 35% for U-2932 and 27% for SU-DHL-4. This was a two- to three-fold increase in degradation above that seen for K7153A alone (Figure 5*B*). The amount of total catabolite produced following treatment was also calculated, taking into account both the quantity of antibody bound and the percent degraded. The amount of ^{3}H-K7153A catabolite ranged from 0.050 to 0.110 pmol degraded antibody per million cells when incubated alone but increased two- to three-fold (0.141-0.223 pmol) when combined with rituximab (Figure 5*C*). Similar experiments showed that the degradation of radiolabeled anti-CD19 antibody was minimally affected by the addition of rituximab and produced considerably less catabolite than the combination of K7153A and rituximab. These results are consistent with the generation of higher concentrations of cytotoxic catabolite as a consequence of increased internalization and degradation of IMGN529 in the presence of rituximab.

Effect of Rituximab on the Antitumor Efficacy of IMGN529 in Multiple B-Cell NHL Xenograft Models

To examine whether the superior antitumor activity of IMGN529 conferred by rituximab cotreatment *in vitro* would translate to

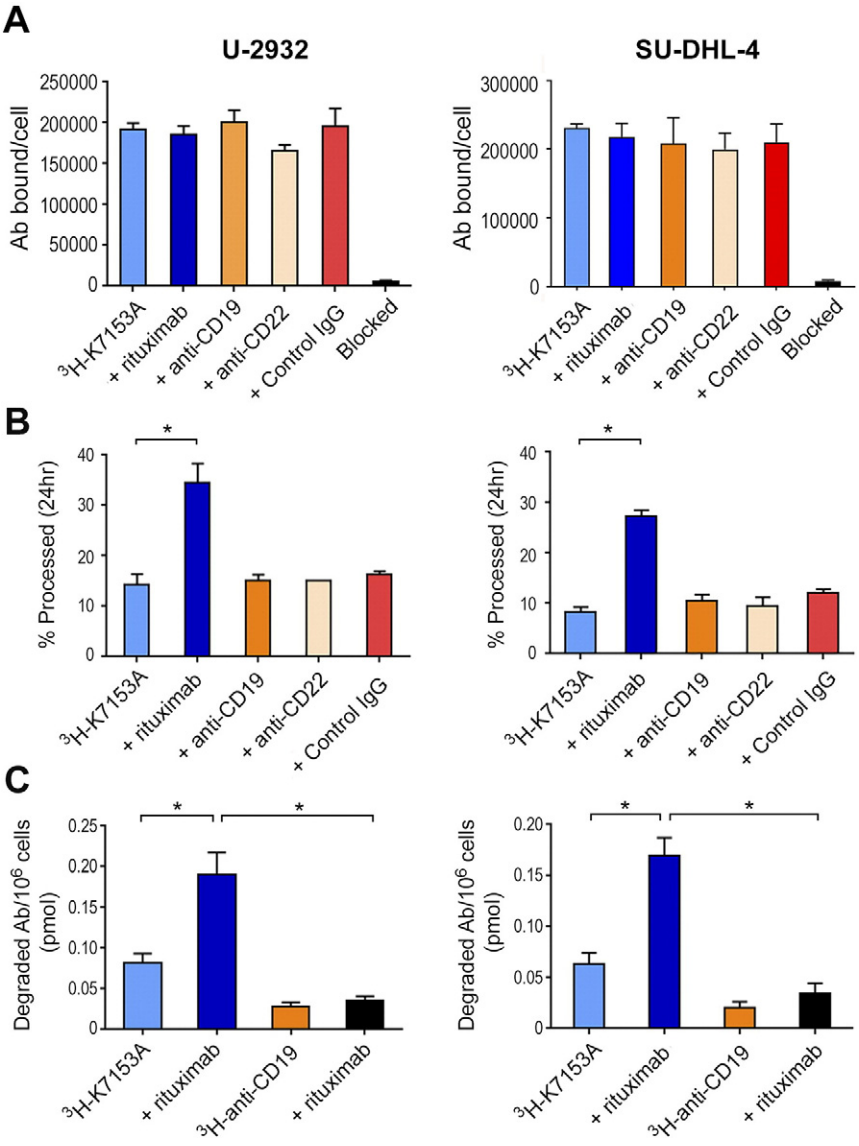

Figure 5. IMGN529 processing and catabolite formation are enhanced in the presence of rituximab. (A) U-2932 (*left panel*) and SU-DHL-4 cells (*right panel*) cells were pulse-treated with 10 nM ^{3}H-K7153A either alone or in the presence of the indicated antibodies (10 nM) for 30 minutes and cultured for 24 hours at 37°C. Antibodies bound per cell values were calculated from resulting total sample CPM using the ^{3}H- K7153A reagent-specific radioactivity, cell number, and assumption of 1:1 reagent per receptor binding. (B) U-2932 and SU-DHL-4 cells were treated with 10 nM of ^{3}H-K7153A either alone or in the presence of the indicated antibodies (10 nM) for 30 minutes and cultured for 24 hours at 37°C. Cells and media were precipitated with acetone upon harvest, and the percentage processed was calculated from the CPM values of the supernatant (processed ^{3}H-7153A) and pellet (intact ^{3}H-7153A) (*P < .0001). (C) The amount of degraded ^{3}H-Ab (catabolite) was calculated from the supernatant (processed ^{3}H-Ab) CPM value and converted to picomoles of catabolite per million cells (*P < .0001).

improved efficacy *in vivo*, mice bearing DLBCL xenografts were treated with IMGN529 and rituximab both as monotherapy and in combination. Representative data of experiments are shown in Figure 6. Mice with U-2932 ABC-DLBCL tumors received a single administration of IMGN529 (10 mg/kg) or three weekly doses (QW×3) of 10 mg/kg rituximab (Figure 6*A*). IMGN529 monotherapy was inactive (63% T/C, 0/8 PR, 0/8 CR, 0/8 TFS) against U-2932 tumors. Rituximab monotherapy was active in this model, but few regressions were observed (1/8 PR, 0/8 CR). Consistent with the *in vitro* findings above, concurrent treatment with both IMGN529 and rituximab resulted in a substantial enhancement of antitumor activity. The combination was highly active (T/C 8%), with multiple regressions (7/8 PR, 6/8 CR) that were durable through the study end on day 90 (6/8 TFS). The efficacy of combination IMGN529 and rituximab was compared to the clinically relevant combination R-CHOP. R-CHOP was also highly active in this model (T/C 9.6%); however, fewer regressions were observed (4/8 PR, 2/8 CR), and regressions were transient (0/8 TFS) unlike the IMGN529 plus rituximab combination. Importantly, the combination of IMGN529 plus rituximab was well tolerated, with no overt toxicity or loss of body weight observed over the course of the study. Next, we evaluated the antitumor activity of IMGN529 and rituximab in GCB-DLBCL xenografts models. Data from a study using the SU-DHL-4 model are shown in Figure 6*B*. Mice received a

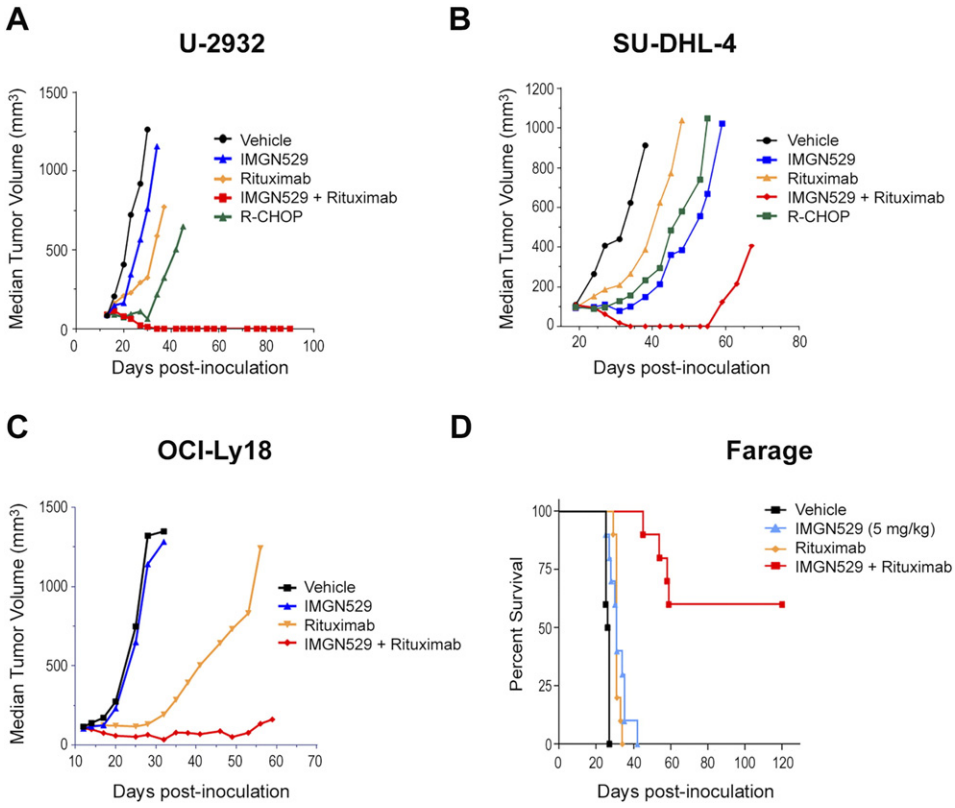

Figure 6. Combination IMGN529 plus rituximab treatment confers superior antitumor efficacy *in vivo* in models of B-cell NHL. (A) SCID mice bearing U-2932 xenografts were dosed with vehicle, R-CHOP, a single dose of 10 mg/kg IMGN529, 10 mg/kg rituximab (QW×3), or the combination. (B) SCID mice bearing SU-DHL-4 xenografts were treated with a single dose of vehicle, R-CHOP, 10 mg/kg IMGN529, 10 mg/kg rituximab, or the combination, as indicated. (C) SCID mice bearing OCI-Ly18 xenografts were treated with a single dose of vehicle, 10 mg/kg IMGN529, 10 mg/kg rituximab, or the combination. (D) Kaplan-Meier analysis of overall survival in the Farage xenograft model. Beginning 7 days after tumor cell inoculation, SCID mice with disseminated lymphatic disease were dosed with vehicle, a single administration of 5 mg/kg IMGN529, 10 mg/kg rituximab (QW×3), or the combination, and animal survival was monitored out to 120 days.

single administration of IMGN529 or rituximab at 10 mg/kg, and each regimen was active (T/C 16% and 42%) with few regressions (2/8 PR, 1/8 CR vs 2/8 PR, 2/8 CR) and TFS at study end (0/8 vs 2/8, respectively). Similar to the findings in the U2932 model, combination therapy consisting of IMGN529 plus rituximab was highly active (T/C 0%) with multiple durable regressions (5/8 PR, 5/8 CR, 4/8 TFS). This combination had enhanced activity when compared to R-CHOP, which was active (25% T/C) with few regressions (2/8 PR, 2/8 CR, 1/8 TFS). Superior combination therapy activity compared to monotherapy IMGN529 or rituximab was also observed in studies using the DOHH-2 GCB-DLBCL subcutaneous xenograft model (data not shown).

DLBCL tumors with genetic alterations in MYC and BCL2 are highly aggressive with a poor prognosis. We evaluated the combination of IMGN529 and rituximab in the MYC/BCL2 double-hit model, OCI-Ly18 (Figure 6*C*). OCI-Ly18 tumors were insensitive to 10 mg/kg IMGN529 (T/C 83%; 0/8 PR, CR, and TFS). Rituximab dosed once at 10 mg/kg was active (T/C of 12%). However, only three of eight mice had partial regressions of their tumors. No complete regressions were observed. Combination IMGN529 plus rituximab was very efficacious against these highly aggressive double-hit tumors. The combination was highly active with a T/C of 5% and, importantly, induced many regressions (6/8 PR) including durable complete regressions (2/8 CR and TFS). In all models, IMGN529, rituximab, and IMGN529 + rituximab treatments were well tolerated, with no significant loss of body weights observed (Supplementary Figure 1).

The Farage GCB-DLBCL cell line was used to evaluate the overall survival benefit of IMGN529 and rituximab in a disseminated lymphoma model. Mice were inoculated with Farage cells, and treatment was initiated 7 days later to ensure engraftment and outgrowth of lymphoma cells. Animals were dosed with either a single administration of IMGN529 (5 mg/kg) or QW×3 rituximab (10 mg/kg), alone and in combination. As shown in the Kaplan-Meier curves (Figure 6*D*), IMGN529 and rituximab monotherapies only slightly extended median survival compared to vehicle-treated animals. However, IMGN529 plus rituximab was highly active, as evidenced by a >350% increased life span and 6 of 10 mice still alive at study end (day 120).

Discussion

Improving outcomes for NHL patients, in particular those with refractory/relapsed DLBCL, remains an ongoing challenge. As evidenced by the clinical success of rituximab, antibody-based therapies are important in the management of a number of hematological malignancies, and in this regard, CD37 represents a promising antigen target for the development of new B-cell–directed therapeutics. IMGN529 is a CD37-targeting ADC that has shown

encouraging signs of activity in early human trials. In this study, we show that combinations of IMGN529 with approved anti-CD20 antibodies, including rituximab, confer superior antitumor activity over IMGN529 alone in preclinical models of DLBCL. Moreover, our findings support a novel mechanism of action to account for enhanced antitumor activity of IMGN529 in the presence of rituximab, whereby CD20 engagement triggers increased internalization and degradation of IMGN529 to release greater amounts of cytotoxic agent.

By screening a library of oncology-related compounds, a variety of agents were uncovered that could enhance the cytotoxic activity of IMGN529. Notably, the strongest synergies were observed with anti-CD20 antibodies, thus identifying a clinically relevant and actionable class of therapeutics for further evaluation. Confirming the results of that assay, cotreatment of IMGN529 with rituximab, ofatumumab, or obinutuzumab was shown to enhance apoptosis across a panel of B-cell NHL lines. *In vitro* cytotoxicity improvements have been reported in NHL when anti-CD20 antibodies are combined with an anti-CD37 scFv-Fc agent (as both a chimeric or humanized fusion protein; SMIP-016 and otlertuzumab, respectively) [22,23]. Based on these data, otlertuzumab plus rituximab is in early-stage clinical evaluation [12]. Unlike IMGN529, the biological activities of these fusion proteins are limited to direct proapoptotic signaling and ADCC induction [9], and indeed, the increased *in vitro* activity of SMIP-016 in the presence of rituximab observed in these studies was a result of enhancement of the intrinsic proapoptotic activity of the CD37-targeting moiety. While our data showed that combination treatment could enhance the proapoptotic activity of the antibody component of IMGN529, the combinatorial benefits with the intact ADC were much greater than those seen with the antibody alone.

Distinct from these other CD37-directed agents, IMGN529 couples the pharmacodynamic effect of targeted delivery of a cancer-killing cytotoxic payload with the functional activities of its antibody component [16]. The full antitumor activity IMGN529 relies on the internalization, intracellular trafficking, and degradation of the ADC molecule in order to release cytotoxic amounts of the maytansinoid payload. Using the antibody (K7153A) that serves as the CD37-targeting portion of IMGN529, we showed that coincubation with rituximab resulted in increased internalization. Further, anti-CD20–mediated enhanced internalization of K7153A appeared to be a class effect because the response was also induced by ofatumumab and obinutuzumab. The lysosomal degradation of radiolabeled K7153A and catabolite formation were also significantly increased in the presence of rituximab but not of a nontargeting control antibody or antibodies directed to the other B-cell antigens: CD19 and CD22. The increase internalization of IMGN529 in the presence of anti-CD20 antibodies was unexpected given that CD37 and CD20 are not known to physically interact nor have overlapping signaling pathways. However, we did show that this effect was not a result of a general disruption in membrane permeability or membrane turnover, as CD20 internalization remained unchanged following treatment. Taken together, these findings provide compelling evidence for a mechanistic model by which CD20 binding promotes increased internalization and degradation of IMGN529, sufficient to generate greater amounts of cytotoxic catabolites.

An important finding of this study was the ability of rituximab to considerably improve the *in vivo* efficacy of single-agent IMGN529 therapy. For two decades now, rituximab has played an indispensable role in NHL treatment, indicated for use both as a single agent and alongside cytoreductive combination chemotherapy, e.g., R-CHOP [24]. As part of an evolution away from chemotherapy-based management of NHL, a number of clinical investigations of rituximab in combination with ADCs directed against other B-cell antigens are being explored [25]. To date, the most advanced of these have involved two CD22-targeting ADCs. The first, inotuzumab ozogamicin (INO), comprises an anti-CD22 antibody to which a calicheamicin payload is attached *via* an acid-labile linker [26]. A phase 1/2 study evaluating the rituximab-INO (R-INO) combination in patients with $CD20^+/CD22^+$ B-cell NHL [27] revealed higher objective response rates and median patient free survival compared to INO monotherapy [28]. However, in a subsequent phase 2 trial in relapsed/refractory DLBCL patients, R-INO therapy had lower than expected activity as a salvage regimen [29], and a phase 3 study evaluating the combination in FL patients was discontinued early due to futility [30]. Pinatuzumab vedotin also targets CD22, but the antibody moiety is conjugated, *via* stable linkage, to MMAE [31]. Recent human trials with this ADC have shown that rituximab can be combined with pinatuzumab vedotin; preliminary efficacy signals suggest an improvement of the combination compared to the ADC alone [32,33]. It is unclear whether the mechanisms involved in the CD20 and CD22 combinations are similar or distinct from those described here for our CD37-targeting ADC.

Conclusion

Collectively, this work demonstrates that CD20 engagement promotes IMGN529 internalization and processing to confer superior antitumor activity in preclinical models and provides a novel mechanistic rationale for the potential clinical benefits of this combination. The ability of a well-established standard-of-care agent to potentiate the activity of IMGN529 suggests that this combination holds considerable promise for the future management of B-cell NHL. The clinical benefit of the combination of IMGN529 and rituximab is currently being examined in a phase 2 study in CD37-positive patients with relapsed or refractory B-cell lymphoma (NCT02564744).

Supplementary data to this article can be found online at http://dx.doi.org/10.1016/j.neo.2017.06.001.

Funding

This research did not receive any grant from funding agencies in the public, commercial, or not-for-profit sectors, with all work funded by ImmunoGen, Inc.

Acknowledgements

We thank the members of the ImmunoGen research team for their contributions to the work presented here. We also thank Dr. Richard Bates who provided drafts and editorial assistance during production of this manuscript.

References

[1] Ku M, Chong G, and Hawkes EA (2017). Tumour cell surface antigen targeted therapies in B-cell lymphomas: beyond rituximab. *Blood Rev* **31**, 23–25.

[2] Maloney DG (2012). Anti-CD20 antibody therapy for B-cell lymphomas. *N Engl J Med* **366**, 2008–2016.

[3] van Spriel AB, Puls KL, Sofi M, Pouniotis D, Hochrein H, Orinska Z, Knobeloch KP, Plebanski M, and Wright MD (2004). A regulatory role for CD37 in T cell proliferation. *J Immunol* **172**, 2953–2961.

[4] Lapalombella R, Yeh YY, Wang L, Ramanunni A, Rafiq S, Jha S, Staubli J, Lucas DM, Mani R, and Herman SE, et al (2012). Tetraspanin CD37 directly mediates transduction of survival and apoptotic signals. *Cancer Cell* **21**, 694–708.

[5] Link MP, Bindl J, Meeker TC, Carswell C, Doss CA, Warnke RA, and Levy R (1986). A unique antigen on mature B cells defined by a monoclonal antibody. *J Immunol* **137**, 3013–3018.

[6] Schwartz-Albiez R, Dorken B, Hofmann W, and Moldenhauer G (1988). The B cell-associated CD37 antigen (gp40-52). Structure and subcellular expression of an extensively glycosylated glycoprotein. *J Immunol* **140**, 905–914.

[7] Barrena S, Almeida J, Yunta M, Lopez A, Fernandez-Mosteirin N, Giralt M, Romero M, Perdiguer L, Delgado M, and Orfao A, et al (2005). Aberrant expression of tetraspanin molecules in B-cell chronic lymphoproliferative disorders and its correlation with normal B-cell maturation. *Leukemia* **19**, 1376–1383.

[8] Moore K, Cooper SA, and Jones DB (1987). Use of the monoclonal antibody WR17, identifying the CD37 gp40-45 Kd antigen complex, in the diagnosis of B-lymphoid malignancy. *J Pathol* **152**, 13–21.

[9] Zhao X, Lapalombella R, Joshi T, Cheney C, Gowda A, Hayden-Ledbetter MS, Baum PR, Lin TS, Jarjoura D, and Lehman A, et al (2007). Targeting CD37-positive lymphoid malignancies with a novel engineered small modular immunopharmaceutical. *Blood* **110**, 2569–2577.

[10] Heider KH, Kiefer K, Zenz T, Volden M, Stilgenbauer S, Ostermann E, Baum A, Lamche H, Kupcu Z, and Jacobi A, et al (2011). A novel Fc-engineered monoclonal antibody to CD37 with enhanced ADCC and high proapoptotic activity for treatment of B-cell malignancies. *Blood* **118**, 4159–4168.

[11] Byrd JC, Pagel JM, Awan FT, Forero A, Flinn IW, Deauna-Limayo DP, Spurgeon SE, Andritsos LA, Gopal AK, and Leonard JP, et al (2014). A phase 1 study evaluating the safety and tolerability of otlertuzumab, an anti-CD37 mono-specific ADAPTIR therapeutic protein in chronic lymphocytic leukemia. *Blood* **123**, 1302–1308.

[12] Gopal AK, Tarantolo SR, Bellam N, Green DJ, Griffin M, Feldman T, Mato AR, Eisenfeld AJ, Stromatt SC, and Goy A (2014). Phase 1b study of otlertuzumab (TRU-016), an anti-CD37 monospecific ADAPTIR therapeutic protein, in combination with rituximab and bendamustine in relapsed indolent lymphoma patients. *Invest New Drugs* **32**, 1213–1225.

[13] Lambert JM (2013). Drug-conjugated antibodies for the treatment of cancer. *Br J Clin Pharmacol* **76**, 248–262.

[14] Katz J, Janik JE, and Younes A (2011). Brentuximab vedotin (SGN-35). *Clin Cancer Res* **17**, 6428–6436.

[15] Lambert JM and Chari RV (2014). Ado-trastuzumab emtansine (T-DM1): an antibody-drug conjugate (ADC) for HER2-positive breast cancer. *J Med Chem* **57**, 6949–6964.

[16] Deckert J, Park PU, Chicklas S, Yi Y, Li M, Lai KC, Mayo MF, Carrigan CN, Erickson HK, and Pinkas J, et al (2013). A novel anti-CD37 antibody-drug conjugate with multiple anti-tumor mechanisms for the treatment of B-cell malignancies. *Blood* **122**, 3500–3510.

[17] Pereira DS, Guevara CI, Jin L, Mbong N, Verlinsky A, Hsu SJ, Avina H, Karki S, Abad JD, and Yang P, et al (2015). AGS67E, an anti-CD37 monomethyl auristatin E antibody-drug conjugate as a potential therapeutic for B/T-cell malignancies and AML: a new role for CD37 in AML. *Mol Cancer Ther* **14**, 1650–1660.

[18] Beckwith KA, Frissora FW, Stefanovski MR, Towns WH, Cheney C, Mo X, Deckert J, Croce CM, Flynn JM, and Andritsos LA, et al (2014). The CD37-targeted antibody-drug conjugate IMGN529 is highly active against human CLL and in a novel CD37 transgenic murine leukemia model. *Leukemia* **28**, 1501–1510.

[19] Stathis A, Freedman AS, Flinn IW, Maddocks KJ, Weitman S, Berdeja JG, Mejia AV, Green R, Romanelli A, and Zildjian SH, et al (2014). A phase I study of IMGN529, an antibody-drug conjugate (ADC) targeting CD37, in adult patients with relapsed or refractory B-cell non-Hodgkin's lymphoma (NHL). *Blood* **124**, 1760 [abstract].

[20] Lai KC, Deckert J, Setiady YY, Shah P, Wang L, Chari R, and Lambert JM (2015). Evaluation of targets for maytansinoid ADC therapy using a novel radiochemical assay. *Pharm Res* **32**, 3593–3603.

[21] Johnson P and Glennie M (2003). The mechanisms of action of rituximab in the elimination of tumor cells. *Semin Oncol* **30**, 3–8.

[22] Baum PR, Cerveny C, Gordon B, Nilsson C, Wiens J, Rafiq S, Lapalombella R, Muthusamy N, Byrd JC, and Wahl A (2009). Evaluation of the effect of TRU-016, an anti-CD37 directed SMIP in combination with other therapeutic drugs in models of non-Hodgkin's lymphoma. *J Clin Oncol* **27**, 8571 [abstract].

[23] Smolewski P, Robak P, Cebula-Obrzut B, Misiewicz M, Medra A, Majchrzak A, Witkowska M, Stromatt S, and Robak T (2014). Pro-apoptotic effect of an anti-CD37 scFv-Fc fusion protein, in combination with the anti-CD20 antibody, ofatumumab, on tumour cells from B-cell malignancies. *Eur J Cancer* **50**, 2677–2684.

[24] Eichenauer DA, Engert A, and Schulz H (2009). Expanded use of rituximab in the management of non-Hodgkin lymphoma. *Onco Targets Ther* **2**, 189–197.

[25] Mehta A and Forero-Torres A (2015). Development and integration of antibody-drug conjugate in non-Hodgkin lymphoma. *Curr Oncol Rep* **17**, 41.

[26] DiJoseph JF, Armellino DC, Boghaert ER, Khandke K, Dougher MM, Sridharan L, Kunz A, Hamann PR, Gorovits B, and Udata C, et al (2004). Antibody-targeted chemotherapy with CMC-544: a CD22-targeted immunoconjugate of calicheamicin for the treatment of B-lymphoid malignancies. *Blood* **103**, 1807–1814.

[27] Fayad L, Offner F, Smith MR, Verhoef G, Johnson P, Kaufman JL, Rohatiner A, Advani A, Foran J, and Hess G, et al (2013). Safety and clinical activity of a combination therapy comprising two antibody-based targeting agents for the treatment of non-Hodgkin lymphoma: results of a phase I/II study evaluating the immunoconjugate inotuzumab ozogamicin with rituximab. *J Clin Oncol* **31**, 573–583.

[28] Advani A, Coiffier B, Czuczman MS, Dreyling M, Foran J, Gine E, Gisselbrecht C, Ketterer N, Nasta S, and Rohatiner A, et al (2010). Safety, pharmacokinetics, and preliminary clinical activity of inotuzumab ozogamicin, a novel immunoconjugate for the treatment of B-cell non-Hodgkin's lymphoma: results of a phase I study. *J Clin Oncol* **28**, 2085–2093.

[29] Wagner-Johnston ND, Goy A, Rodriguez MA, Ehmann WC, Hamlin PA, Radford J, Thieblemont C, Suh C, Sweetenham J, and Huang Y, et al (2015). A phase 2 study of inotuzumab ozogamicin and rituximab, followed by autologous stem cell transplant in patients with relapsed/refractory diffuse large B-cell lymphoma. *Leuk Lymphoma* **56**, 2863–2869.

[30] Pfizer discontinues phase 3 study of inotuzumab ozogamicin in relapsed or refractory aggressive non-Hodgkin lymphoma (NHL) due to futility. Pfizer, Inc.; 2013 [http://press.pfizer.com/press-release/pfizer-discontinues-phase-3-study-inotuzumab-ozogamicin-relapsed-or-refractory-aggress].

[31] Li D, Poon KA, Yu SF, Dere R, Go M, Lau J, Zheng B, Elkins K, Danilenko D, and Kozak KR, et al (2013). DCDT2980S, an anti–CD22-monomethyl auristatin E antibody-drug conjugate, is a potential treatment for non-Hodgkin lymphoma. *Mol Cancer Ther* **12**, 1255–1265.

[32] Advani RH, Lebovic D, Chen A, Brunvand M, Goy A, Chang JE, Hochberg E, Yalamanchili S, Kahn R, and Lu D, et al (2017). Phase I study of the anti-CD22 antibody-drug conjugate pinatuzumab vedotin with/without rituximab in patients with relapsed/refractory B-cell non-Hodgkin lymphoma. *Clin Cancer Res* **23**, 1167–1176.

[33] Morschhauser F, Flinn IW, Advani RH, Sehn LH, Kolibaba KS, Press OW, Salles GA, Magid Diefenbach CS, Tilly H, and Assouline SE, et al (2014). Preliminary results of a phase II randomized study (ROMULUS) of polatazumab vedotin or pinatuzumab vedotin plus rituximab in patients with relapsed/refractory (R/R) non-Hodgkin lymphoma. *J Clin Oncol* **32**, 8519 [abstract].